Title

Ex-vivo imaging and plaque type classification of intracranial atherosclerotic plaque using high resolution MRI

Permalink

https://escholarship.org/uc/item/23x4k29d

Authors

Jiang, Yuanliang
Zhu, Chengcheng
Peng, Wenjia
et al.

Publication Date

2016-06-01

DOI

10.1016/j.atherosclerosis.2016.03.033

Peer reviewed

Ex-vivo Imaging and Plaque Type Classification of Intracranial Atherosclerotic Plaque using High Resolution MRI

Yuanliang Jiang, MD[1,*], **Chengcheng Zhu, PhD**[2,*,†], **Wenjia Peng, MD**[1], **Andrew J. Degnan, MD**[3], **Luguang Chen, MSc**[1], **Xinrui Wang, MD**[1], **Qi Liu, MD**[1], **Yang Wang, MD**[4], **Zhenzhen Xiang, MD**[4], **Zhongzhao Teng, PhD**[5], **David Saloner, PhD**[2], and **Jianping Lu, MD**[1,†]

[1]Department of Radiology, Changhai Hospital, Shanghai, China

[2]Department of Radiology and Biomedical Imaging, UCSF, San Francisco, CA, USA

[3]Department of Radiology, University of Pittsburgh, Pittsburgh, USA

[4]Department of Pathology, Changhai Hospital, Shanghai, China

[5]Department of Radiology, University of Cambridge, Cambridge, UK

Abstract

Background and Aims—Recent development of high resolution MRI techniques have enabled imaging of intracranial atherosclerotic plaque *in vivo*. However, identifying plaque composition remains challenging given the small size and the lack of histological validation. This study aims to quantify the relaxation times of intracranial plaque components *ex vivo* at 3T and to determine whether multi-contrast MRI could classify intracranial plaque according to the American Heart Association classification with histological validation.

Methods—A total of 53 intracranial arteries with atherosclerotic plaques from 20 cadavers (11 male, age 73.8±10.9) were excised. Quantitative $T_1/T_2/T_2^*$ mapping sequences and multi-contrast fast-spin echo sequences (T_1, T_2, proton-density weighted and short time inversion recovery) were acquired. Plaque components including: fibrous cap, lipid core, fibrous tissue, calcification, and healthy wall were segmented on histology, and their relaxation times were derived from quantitative images. Two radiologists independently classified plaque type blinded to the histology results.

Results—Relaxation times of plaque components are distinct and different. T_2 and T_2^* values of lipid core are lower than fibrous cap (p=0.026 & p<0.0001), but are comparable with fibrous tissue and healthy wall (p=0.76 & p=0.42). MRI reliably classified plaque type compared with histology

---

[†]Corresponding authors: Dr. Chengcheng Zhu, Department of Radiology and Biomedical Imaging, UCSF, San Francisco, CA, USA, 94121, Phone/Fax: +1 415 221 4810 x 3818, ; Email: Chengcheng.Zhu@ucsf.edu, Prof. Jianping Lu, Department of Radiology, Changhai Hospital, 168 Changhai Road, Shanghai, China, 200433, Phone/Fax: +86-21-81873226, ; Email: cjr.lujianping@vip. 163.com
[*]Contribute equally

(κ=0.69) with an overall accuracy of 80.7%. The sensitivity and specificity using MRI to identify fibro-lipid atheroma (type IV–V) was 94.8% and 77.1%, respectively. Inter-observer agreement was excellent (κ=0.77).

Conclusion—Intracranial plaque components have distinct and different relaxation times at 3T. High-resolution MRI is able to characterize intracranial plaque composition and classify plaque types ex vivo at 3T.

Keywords

Magnetic Resonance Imaging; Atherosclerosis; Stroke; Ex-vivo; Vessel Wall Imaging

Introduction

Intracranial atherosclerotic disease (ICAD) is increasingly recognized as a major cause of stroke[1] with a recent study observing intracranial stenosis or occlusion in approximately 39% of patients presenting with stroke or transient ischemic attack [2]. Current management of patients with intracranial atherosclerotic plaque relies on assessment of the extent of arterial stenosis. Treatment options for ICAD remain controversial, however, with the benefits of stenting called into question by the SAMMPRIS trial showing poorer outcomes with stenting compared with optimal medical management [3]. It is possible that luminal narrowing alone may fail to provide sufficient information regarding the underlying pathology of the vessel wall and future risk of infarct. Recent development of high resolution MRI techniques have enabled visualization of the intracranial vessel wall in vivo[4–6] . Plaque features including contrast enhancement and intraplaque hemorrhage (IPH) have been found to be possibly linked with neurological symptoms [7–8] and plaque wall imaging has been shown to be complementary to luminal stenosis in defining patient clinical presentations [9]. Further development of intracranial vessel wall imaging may therefore improve our understanding of the risks of specific atherosclerotic lesion types.

Extensive experience from the carotid atherosclerosis imaging literature has established multi-parametric imaging as a means of non-invasively characterizing atherosclerotic plaque[10] with reference to the detailed classification scheme of the American Heart Association (AHA) that was established to grade plaque properties[11] Extracranial carotid plaque components such as IPH, fibrous cap and lipid core have been extensively studied as predictors of ischemic stroke [10]. Characterizing intracranial plaque composition *in vivo*, however, is still challenging given the small size and the lack of histological validation of those lesions [12–14] . Whether clinical MRI can provide sufficient soft tissue contrast to differentiate intracranial plaque components remains largely unproven.

$T_1/T_2/T_2^*$ relaxation times are the basis of MRI for generating tissue contrast that can provide information on plaque properties. Previous post-mortem studies have reported relaxation times of intracranial plaque components at ultra-high field strengths (7T[15] and 17.6T[16]). However, most prior *in vivo* studies of intracranial plaque were undertaken using 3T clinical scanners which are widely available [4–8] , but relaxation times at 3T have not yet been reported.

This study aims to quantify the MRI relaxation times of intracranial plaque components ex vivo at 3T and to evaluate the ability of multi-contrast MRI for classifying intracranial plaque types ex vivo[17] with histological validation.

Methods

Study population

The study was conducted following approval of Shanghai Changhai Hospital Ethics Committee (approval identifier: CHEC2013-204). Written informed consent was obtained from all patients or patients' family members. Specimens of the circle of Willis (CoW) were obtained from 20 cadavers identified with intracranial atherosclerotic plaques at Changhai Hospital, Shanghai, China, from January 2013 to June 2015. Of these cadavers 11 were males and 9 females and the mean age was 73.8 ± 10.9 years. The cause of death included multiple organ failure (n=8), acute myocardial infarction (n=1), pulmonary embolus (n=2), aortic dissection (n=1), aortic aneurysm rupture (n=1), pneumonia (n=1), cardiovascular and cerebrovascular diseases (n=3), and unknown (n=3). All specimens were rinsed with saline to remove blood clots.

MRI Protocol

MRI scanning was undertaken in a 3T whole body system (MAGNETOM Skyra, Siemens Healthcare, Erlangen, Germany) using a loop coil (4cm diameter) within 24 hours after excising specimen. During imaging, specimens were embedded within Fomblin (Solvey Solexis, Milan, Italy) which is a fluorinated fluid with no MR signal. Quantitative $T_1/T_2/T_2^*$ mapping sequences (qT_1, qT_2, qT_2^*) and multi-contrast fast-spin echo (FSE) sequences including T_1, T_2, proton-density (PD) weighted and short inversion time recovery (STIR) were acquired transverse to the axis of the arterial segments. The specimen was fixed during the entire scan and the sequences were prescribed at the same locations. Scanning parameters are summarized in Table 1. An inversion recovery (IR) gradient echo (GRE) sequence with 5 inversion times (TIs) was used for T_1 mapping; a FSE sequence with 5 echoes was used for T_2 mapping; and a multi-echo GRE sequence with 5 echoes was used for T_2^* mapping. The proton density values of plaque components were also quantified by normalizing the signal intensities on PD-weighted images, with the signal intensities of the healthy wall set to 1 as a reference.

There was a difference in the resolution of quantitative parameter mapping sequences, which was limited by the MRI sequences available (Siemens product sequences that are designed for clinical use), the small field of view (2.9cm to 7cm) and the scanner's hardware performance (maximal gradient amplitude and slew rate).

The entire scan took 57 minutes 43 seconds to 3 hours 26 minutes and 14 seconds depending on the number of slices imaged (Table 1). The scan time was considerably shorter than in previous ex-vivo studies [12–13]. Therefore, we assumed the relaxation properties of the plaque did not change significantly during the scan.

Histology

The specimens were fixed in formal saline (10% formalin in 0.9% NaCI) for 24 hours following imaging acquisition. After decalcification, samples were cut into 4–5mm blocks and they were numbered to enable coregistration. The arteries were then sectioned at 5 micron thickness every 0.5mm. Sections were stained with haematoxylin-eosin (H&E) and Masson trichrome. The histology sections were digitized using an electronic microscope at 20× magnification (Olympus BX53 microscope, Olympus, Tokyo, Japan). Histology images were examined using standard histopathologic criteria[11]

Image analysis

An experienced radiologist matched the MRI slices with histological sections carefully according to their locations. The gross morphological features including vessel size, shape and calcification were also considered during the co-registration. Plaque components including IPH, fibrous cap, lipid core, fibrous tissue, calcification and healthy wall were identified on histology images. Based on the histological results, region of interests (ROIs) were drawn manually on the corresponding regions on the T_2-weighted images using CMRtools software (Cardiovascular Imaging Solutions Ltd, London, UK). Then the ROIs were copied to the same slices on qT_1, qT_2 and qT_2* images. The relaxation times of different plaque components were recorded.

Plaque types were classified on histology by two experienced pathologists according to the modified AHA plaque type criteria [17]: Type I,II: near normal wall thickness; Type III: diffuse intimal thickening or small eccentric plaque with no calcification; Type IV–V: plaque with a lipid or necrotic core surrounded by fibrous tissue with possible calcification; Type VI: complex plaque with possible surface defect, hemorrhage, or thrombus; Type VII: calcified plaque; Type VIII: fibrotic plaque without lipid core and with possible small calcifications.

Two radiologists also classified the plaque types based on the signal characteristics on multi-contrast MRI [17] blinded to the histology results. As the relaxation times of intracranial plaque components were found to be comparable with previously reported relaxation times of carotid plaque components, the same criteria were used in this study [17].

Statistics

Data were analyzed by using MedCalc software (version 13.3.0.0, MedCalc Software, Belgium). Categorical data were presented as counts, and continuous variables were presented as mean ± standard deviation (SD). Considering that multiple measurements were obtained from each subject, a linear mixed-effect model was used to assess the difference between the relaxation times of different components. Cohen's kappa (κ) was used to estimate the agreement of plaque type classification using MRI compared with histology, and the agreement between observers. Kappa values less than 0.4 were characterized as poor; values of 0.4–0.75 were characterized as fair to good; and values greater than 0.75 were considered excellent [18]. A p-value of less than 0.05 was considered significant. All p-values were 2-sided.

Results

In total, 53 intracranial arteries with atherosclerotic plaques were excised, including 27 middle cerebral arteries (MCAs), 11 basilar arteries (BAs), 4 posterior cerebral arteries (PCAs), 5 anterior cerebral arteries (ACAs), 5 vertebral arteries (VAs) and 1 intracranial carotid artery (ICA). Numbers of plaques and slices selected from each cadaver are shown in supplementary Table S1. Four cadavers were excluded due to absence of plaque and one cadaver was excluded due to inconsistent MRI scanning parameters. As a result, 15 cadavers were included in the analysis. The median number of plaque per patient is 3(inter-quartile range, 2–5) and the median slice number per plaque is 4 (inter-quartile range, 2–6). In 276 slices with matched MRI and histology locations, 69 slices were excluded due to: no presentation of plaque (n=15); error in matching histology and MRI (n=20); damaged or distorted histology (n=19) and poor MRI image quality (n=15). After excluding these cases, 207 slices were included in the final analysis. Lipid core, fibrous cap, fibrous tissue, healthy wall, and calcification were identified. No IPH was observed.

Quantitative Imaging

Quantitative mapping images of the specimens and the corresponding histology is shown in Figure 1&2. Relaxation times and proton densities of intracranial plaque components are summarized in Table 2. There are significant differences among the relaxation times of different plaque components ($p<0.05$). Lipid core has significantly lower T_2 and T_2^* values compared to fibrous cap (p=0.026 & p<0.0001) and has comparable values to fibrous tissue and healthy vessel wall (p=0.76 & p=0.42). Lipid core has lower proton densities compared with fibrous tissue and fibrous cap (p=0.0006 & p<0.0001), and is comparable with healthy wall (p=0.34). T_1 relaxation time of lipid core is shorter compared to fibrous tissue/cap and healthy wall (p=0.01, p<0.0001 and p=0.0026). Fibrous cap has the highest relaxation times and proton density, while calcification has the lowest values.

AHA Plaque Type Classification and Inter-observer Agreement

Multi-contrast MRI and corresponding histology images are shown in Figures 1&2. The agreement between MRI and histology for AHA plaque type classification is shown in Table 3 (reader 1) and Table S2 (reader 2); and the inter-observer agreement using MRI for classification is shown in Table 4.

No complex plaque type with fibrous cap rupture or IPH (type VI) was identified on histology. Most plaques were fibro-lipid atheroma (type IV–V, 95/207), followed by diffuse wall thickening (type III, 69/207) and fibrotic atheroma (19/207).

There is excellent inter-observer agreement ($\kappa = 0.77$) between two radiologists for plaque classification with an overall agreement of 85.5%. Inter-observer agreement is generally good to excellent for most plaque types except for a lower agreement for type VIII plaques.

Because the inter-observer agreement was excellent, only the results from reader 1 are summarized below. Multi-contrast MRI shows a good agreement with histology for plaque type classification with κ value of 0.69, and an overall agreement of 80.7%. The sensitivities and specificities using MRI to identify each plaque type are: Type I-II: 61.5% and 100%;

Type III: 77.6% and 83.9%; Type IV–V: 94.8% and 77.1%; Type VII: 100% and 100%; Type VIII: 31.6% and 66.7%. MRI can reliably detect most plaque types except for fibrotic atheroma (type VIII). In identifying high risk fibro-lipid atheroma, MRI has excellent specificity (95.8%) and good sensitively (77.1%).

Discussion

To our knowledge, this is the first study to report the *ex vivo* relaxation times of intracranial plaque components at 3T. The study shows that 3T MRI has the potential to identify intracranial lesion types noninvasively. Distinct and different relaxation times of plaque components are noted. It also demonstrated that multi-contrast MRI at 3T is capable of classifying plaque types reliably with good agreement with histology. The knowledge of relaxation times for major plaque components is essential for understanding the signal characteristics of intracranial plaque *in vivo*. The reported relaxation times can be used in protocol design/optimization and for the characterization of plaque components on multi-contrast imaging at 3T. Characterization of intracranial plaque is becoming increasingly important clinically with the recognition of ICAD as a major contributor to stroke risk worldwide.

Most previous *in vivo* studies of the intracranial vessel wall have used clinical 3T scanners [4–8], and only very few studies have used research 7T scanners due to limited availability [19–20]. Some 3T studies found heterogeneous plaque signal properties on T_1/T_2 weighted images possibly associated with brain infarct patterns [21] or neurological symptoms [9]. The observed heterogeneous signals may indicate different plaque composition; however, these assumptions are still tenuous without histological validation. Comparison between MRI and histology is still rare at 3T except in one case report [14].

Histological validation has been attempted at ultra-high fielded strengths (>=7T) due to the excellent resolution and SNR, and the relaxation times of plaque components have been reported at 7T [15] and 17.4T [16]. However, these results cannot be directly translated to 3T due to the known difference of relaxation times at different field strengths. Therefore, there is an important need to quantify the relaxation times of plaque components at 3T and validate current multi-contrast protocols against histology in order to provide a reference for current 3T *in vivo* studies.

Lipid core was found to have significantly lower T_2 and T_2* values than fibrous cap, such that they could be clearly distinguished on T_2 weighted images. These findings agree well with previous carotid studies at 3T with comparable T_2 values [22]. Such distinct tissue contrast leads to a high specificity and sensitivity for identifying fibro-lipid atheroma (type IV–V) using multi-contrast MRI. T_2 values of lipid core and fibrous cap reported at ultra-high filed strength (15ms to 30ms) [15][16] are significantly lower than at 3T in this study (69ms to 99ms). The drop of T_2 values at higher field strength is well known and attributed to a stronger magnetic susceptibility. However, these high-field studies failed to show a significant difference between the T_2 values of fibrous cap and lipid core. This is possibly due to their small sample size and the relaxation time alterations at higher field strength. Future larger scale studies are needed to confirm these findings. Differences in T_1 and PD

values were also observed among plaque components, however, the best contrast was noted in T_2-weighted images. This is because the ability of each unique sequence is also determined by the strength of the specific weighting and its signal to noise ratio (SNR) performance. STIR has a strong T_2 contrast, but the low SNR is a major limitation. T_1-weighted and proton density-weighted fast-spin-echo imaging have long echo trains and induce considerable T_2 weighting. T_2-weighted imaging has inherently good T_2 weighting and SNR. Therefore, T_2-weighted imaging had the best ability to differentiate lipid core and fibrous cap.

Current *in vivo* resolution (around 0.4mm in plane and 2mm slice thickness) is still substantially lower than the *ex-vivo* resolution in this study (0.1mm in plane and 1mm slice thickness, 1/32 of the *in vivo* voxel size). In addition, a specific loop coil was used in the ex-vivo study, and it had superior SNR performance compared to the standard head coil used in *in vivo* scanning. Therefore, current *in vivo* capacity is still limited in characterizing small plaque components including calcification and thin fibrous cap. However, it may be possible to identify some major features such as a large lipid core (hypointense on T_2-weighted imaging). Recent technical development in 3D high resolution MRI (as low as 0.4mm-0.5mm isotropic) [7] may also improve the sensitivity of current *in vivo* method.

No complex plaque (type VI, fibrous cap rupture or IPH) was identified in this study. This is possibly because there were relatively few patients who died of acute stroke in our study population. A previous in vivo study also reported a low prevalence (10.1%) of IPH (assumed as hyperintense signal in T_1 weighted images) even in patients with severely stenotic MCA plaque [9, 23]. Similarly, IPH was rarely reported in previous post-mortem studies [12–13, 16]. More fundamentally, the lack of IPH may reflect differences in the pathophysiology of intracranial atherosclerotic disease compared to carotid atherosclerosis, which has been examined in greater detail. A recent review of intracranial atherosclerosis pathophysiology suggests that that intracranial lesions show more fibrosis, small lipid pools, and low-grade inflammation in contradistinction to the eroded and ruptured plaque more commonly encountered in extra-cranial atherosclerosis [24]. This difference in pathophysiology of ICAD may explain the low rates of IPH observed in the present study.

The low prevalence of IPH in this study also indicates that ischemic events may be caused by other plaque types such as type IV–V, which is most prevalent in this study (46%). Large lipid core and thin fibrous cap in carotid plaque have been proved to predict future stroke [10]. We demonstrated that multi-contrast MRI can accurately identify the vulnerable fibro-lipid atheroma from low risk plaque types (Type I-II, Type III, Type VII and Type VIII). Only 4.2% of high risk plaques were miss-classified as low risk plaque on MRI in our study. MRI showed a low sensitivity for plaque type VIII identification, and most type VIII plaque were misclassified as type IV–V. This inaccuracy may be due to the appearance of loose fibrous tissue on MRI as heterogeneous signal that may mimic lipid core.

Previously underestimated in European and North American populations, the prevalence of intracranial atherosclerotic disease has become increasingly recognized by non-invasive imaging including CT angiography and MRI as a major contributor to stroke risk beyond extra-cranial, carotid atherosclerotic disease [2]. Unfortunately, management of intracranial

atherosclerotic disease remains problematic on the basis of intracranial stenosis alone. Greater knowledge regarding the risk of plaque progression or infarct occurrence on the basis of plaque composition may be helpful for an improved management strategy. Early studies of interventional techniques in ICAD have demonstrated mixed results; the first prospective study of its kind looking at Wingspan stent placement, SAMMPRIS, observed high complication rates in the stent placement group compared with aggressive medical management with 30 day stroke or death rates of 14.7% versus 5.8% [3]. A more recent retrospective, multi-center trial suggests some benefit for selected populations; the investigators note that stenting of hypoperfused, symptom-associated stenosis is more beneficial than stenting of non-hypoperfused symptomatic stenosis, which carried higher risk of poor outcomes following stenting[25] . Nevertheless, significant risks are incurred in stenting intracranial atherosclerotic lesions and no prospective trials have shown clear benefit to-date [3]. Medical management, however, appears promising with an angiographic study reporting the majority (79%) of stenosis regressing or remaining stable with aggressive medical management, although no definite clinical benefit was observed in this small study [26]. The ability of MRI to identify high-risk plaque features may be able to guide treatment selection as the benefits of each management approach become better understood. A study assessing stable and unstable MCA plaque using MRI observed such artery-to-artery embolic infarction in patients with vulnerable symptomatic MCA plaque, highlighting the possible utility of intracranial vessel MRI in plaque risk assessment [21]. As with carotid atherosclerosis, early evidence examining intracranial plaque with contrast-enhanced MRI suggested an elevated risk of ischemic stroke in patients with inflamed plaque as indicated by enhancement [27]. More recent larger studies confirmed that intracranial plaque enhancement was independently associated with stroke recurrence with a hazard ratio of 7.42 in one study [28] and enhancement was associated with culprit plaque with an odds ratio of 34.6 in another study[7] . Therefore, while plaque risk estimation remains challenging and further work is needed to ascertain the validity of risk estimation based on features other than plaque enhancement, early studies investigating intracranial atherosclerosis plaque imaging show promise for MRI in improving our understanding of pathophysiology and have the potential to better assess risk and direct therapy. The use of clinical MRI of intracranial atherosclerosis needs to be investigated in the future with larger, prospective longitudinal clinical studies. Such trials attempting to correlate plaque properties with long-term outcomes could possibly change the diagnosis and management of intracranial atherosclerotic disease.

Limitations of this study include: 1) No patients' traditional risk factors (Hypertension, Smoking, Hyperlipidemia, etc.) were reported in our study population due to the restrictions of our local IRB; 2) This is an ex-vivo study, so the quantitative relaxation times need to be used with caution when applying into *in vivo* imaging; 3) IPH was not observed in our study population, and future study including high risk patients is needed to report its relaxation times.

Conclusion

Intracranial plaque components have distinct and different relaxation times at 3T. High-resolution MRI is able to characterize intracranial plaque composition and classify plaque

types ex vivo at 3T. This study provides a basis for the development of in vivo MRI techniques to evaluate intracranial plaque vulnerability and improve risk stratification of patients, which may be helpful in the future in guiding management decisions.

Supplementary Material

Refer to Web version on PubMed Central for supplementary material.

Acknowledgments

References

1. Gorelick PB, Wong KS, Bae HJ, Pandey DK. Large artery intracranial occlusive disease: A large worldwide burden but a relatively neglected frontier. Stroke. 2008; 39:2396–2399. [PubMed: 18535283]

2. Mattioni A, Cenciarelli S, Biessels G, van Seeters T, Algra A, Ricci S. Prevalence of intracranial large artery stenosis and occlusion in patients with acute ischaemic stroke or tia. Neurol Sci. 2014; 35:349–355. [PubMed: 23959530]

3. Chimowitz MI, Lynn MJ, Derdeyn CP, Turan TN, Fiorella D, Lane BF, et al. Stenting versus aggressive medical therapy for intracranial arterial stenosis. N Engl J Med. 2011; 365:993–1003. [PubMed: 21899409]

4. Xu WH, Li ML, Gao S, Ni J, Zhou LX, Yao M, et al. Plaque distribution of stenotic middle cerebral artery and its clinical relevance. Stroke. 2011; 42:2957–2959. [PubMed: 21799160]

5. Qiao Y, Steinman DA, Qin Q, Etesami M, Schar M, Astor BC, et al. Intracranial arterial wall imaging using three-dimensional high isotropic resolution black blood mri at 3.0 tesla. J Magn Reson Imaging. 2011; 34:22–30. [PubMed: 21698704]

6. Zhang X, Zhu C, Peng W, Tian B, Chen L, Teng Z, et al. Scan-rescan reproducibility of high resolution magnetic resonance imaging of atherosclerotic plaque in the middle cerebral artery. PLoS One. 2015; 10:e0134913. [PubMed: 26247869]

7. Qiao Y, Zeiler SR, Mirbagheri S, Leigh R, Urrutia V, Wityk R, et al. Intracranial plaque enhancement in patients with cerebrovascular events on high-spatial-resolution mr images. Radiology. 2014; 271:534–542. [PubMed: 24475850]

8. Swartz RH, Bhuta SS, Farb RI, Agid R, Willinsky RA, Terbrugge KG, et al. Intracranial arterial wall imaging using high-resolution 3-tesla contrast-enhanced mri. Neurology. 2009; 72:627–634. [PubMed: 19221296]

9. Teng Z, Peng W, Zhan Q, Zhang X, Liu Q, Chen S, et al. An assessment on the incremental value of high-resolution magnetic resonance imaging to identify culprit plaques in atherosclerotic disease of the middle cerebral artery. Eur Radiol. 2015

10. Underhill HR, Hatsukami TS, Fayad ZA, Fuster V, Yuan C. Mri of carotid atherosclerosis: Clinical implications and future directions. Nat Rev Cardiol. 2010; 7:165–173. [PubMed: 20101259]

11. Stary HC, Chandler AB, Dinsmore RE, Fuster V, Glagov S, Insull W Jr, et al. A definition of advanced types of atherosclerotic lesions and a histological classification of atherosclerosis. A report from the committee on vascular lesions of the council on arteriosclerosis, american heart association. Arterioscler Thromb Vasc Biol. 1995; 15:1512–1531. [PubMed: 7670967]

12. van der Kolk AG, Zwanenburg JJ, Denswil NP, Vink A, Spliet WG, Daemen MJ, et al. Imaging the intracranial atherosclerotic vessel wall using 7t mri: Initial comparison with histopathology. AJNR Am J Neuroradiol. 2015; 36:694–701. [PubMed: 25477359]

13. Majidi S, Sein J, Watanabe M, Hassan AE, Van de Moortele PF, Suri MF, et al. Intracranial-derived atherosclerosis assessment: An in vitro comparison between virtual histology by intravascular ultrasonography, 7t mri, and histopathologic findings. AJNR Am J Neuroradiol. 2013; 34:2259–2264. [PubMed: 23811977]

14. Turan TN, Rumboldt Z, Granholm AC, Columbo L, Welsh CT, Lopes-Virella MF, et al. Intracranial atherosclerosis: Correlation between in-vivo 3t high resolution mri and pathology. Atherosclerosis. 2014; 237:460–463. [PubMed: 25463074]

15. Harteveld AA, Denswil NP, Siero JC, Zwanenburg JJ, Vink A, Pouran B, et al. Quantitative intracranial atherosclerotic plaque characterization at 7t mri: An ex vivo study with histologic validation. AJNR Am J Neuroradiol. 2015

16. Zhang S, Yahagi K, Liu L, Xu J, Kolodgie FD, Virmani R, et al. Ultrahigh-resolution mri imaging of intracranial atherosclerosis at 17.6 tesla: An ex vivo study with histological comparison. Proc. Intl. Soc. Mag. Reson. Med. 2015; 23:0553.

17. Cai JM, Hatsukami TS, Ferguson MS, Small R, Polissar NL, Yuan C. Classification of human carotid atherosclerotic lesions with in vivo multicontrast magnetic resonance imaging. Circulation. 2002; 106:1368–1373. [PubMed: 12221054]

18. Fleiss, J. Statistical methods for rates and proportions. New York, NY: Wiley; 1981.

19. van der Kolk AG, Hendrikse J, Brundel M, Biessels GJ, Smit EJ, Visser F, et al. Multi-sequence whole-brain intracranial vessel wall imaging at 7.0 tesla. Eur Radiol. 2013

20. van der Kolk AG, Zwanenburg JJ, Brundel M, Biessels GJ, Visser F, Luijten PR, et al. Intracranial vessel wall imaging at 7.0-t mri. Stroke. 2011; 42:2478–2484. [PubMed: 21757674]

21. Kim JM, Jung KH, Sohn CH, Moon J, Han MH, Roh JK. Middle cerebral artery plaque and prediction of the infarction pattern. Arch Neurol. 2012; 69:1470–1475. [PubMed: 22910889]

22. Biasiolli L, Lindsay AC, Chai JT, Choudhury RP, Robson MD. In-vivo quantitative t2 mapping of carotid arteries in atherosclerotic patients: Segmentation and t2 measurement of plaque components. J Cardiovasc Magn Reson. 2013; 15:69. [PubMed: 23953780]

23. Xu WH, Li ML, Gao S, Ni J, Yao M, Zhou LX, et al. Middle cerebral artery intraplaque hemorrhage: Prevalence and clinical relevance. Ann Neurol. 2012; 71:195–198. [PubMed: 22367991]

24. Ritz K, Denswil NP, Stam OC, van Lieshout JJ, Daemen MJ. Cause and mechanisms of intracranial atherosclerosis. Circulation. 2014; 130:1407–1414. [PubMed: 25311618]

25. Alexander MD, Meyers PM, English JD, Stradford TR, Sung S, Smith WS, et al. Symptom differences and pretreatment asymptomatic interval affect outcomes of stenting for intracranial atherosclerotic disease. AJNR Am J Neuroradiol. 2014; 35:1157–1162. [PubMed: 24676000]

26. Leung TW, Wang L, Soo YO, Ip VH, Chan AY, Au LW, et al. Evolution of intracranial atherosclerotic disease under modern medical therapy. Ann Neurol. 2015; 77:478–486. [PubMed: 25557926]

27. Skarpathiotakis M, Mandell DM, Swartz RH, Tomlinson G, Mikulis DJ. Intracranial atherosclerotic plaque enhancement in patients with ischemic stroke. AJNR Am J Neuroradiol. 2013; 34:299–304. [PubMed: 22859280]

28. Kim JM, Jung KH, Sohn CH, Moon J, Shin JH, Park J, et al. Intracranial plaque enhancement from high resolution vessel wall magnetic resonance imaging predicts stroke recurrence. Int J Stroke. 2016; 11:171–179. [PubMed: 26783308]

Highlights

1. Relaxation times of *ex-vivo* intracranial plaque are firstly reported at 3T.

2. Intracranial plaque components have distinguished relaxation times at 3T.

3. 3T MRI can classify intracranial plaque type reliably *ex-vivo*.

4. This study provides a basis for *in vivo* MRI of intracranial plaque at 3T.
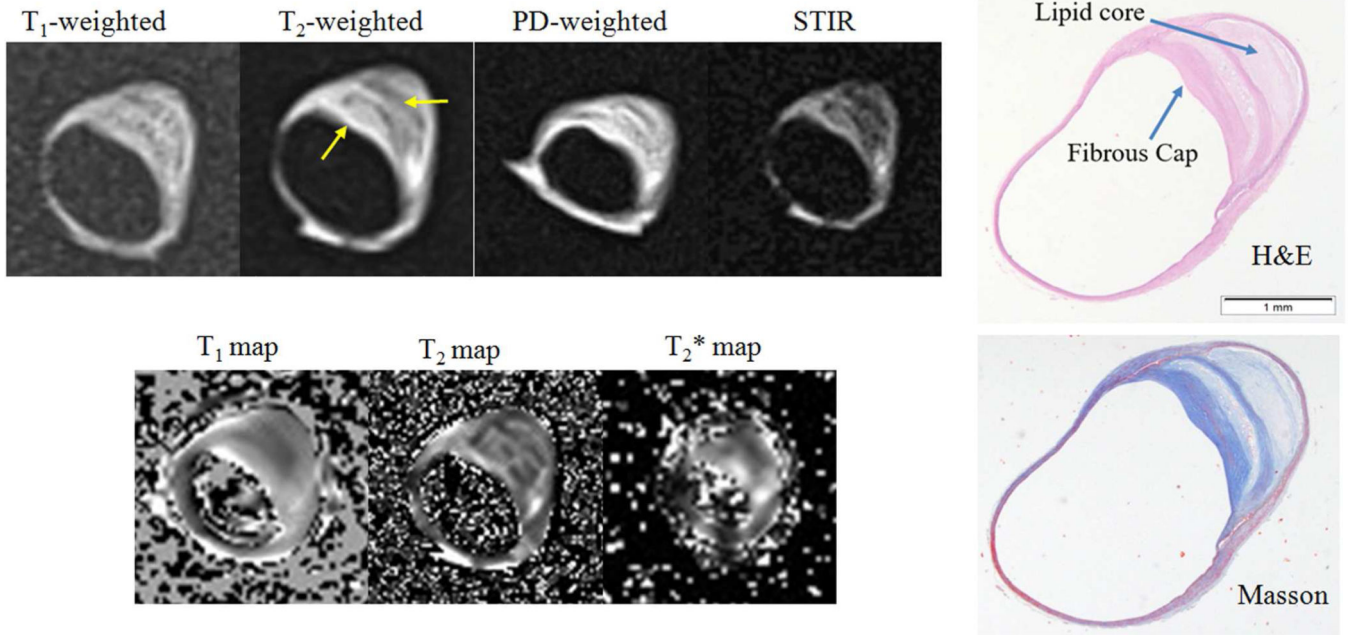
Figure 1.
A middle cerebral artery (MCA) plaque with a thick fibrous cap and a large lipid core (type IV–V). Arrows show the plaque components. PD: proton density; STIR: short time inversion recovery. H&E: haematoxylin - eosin.
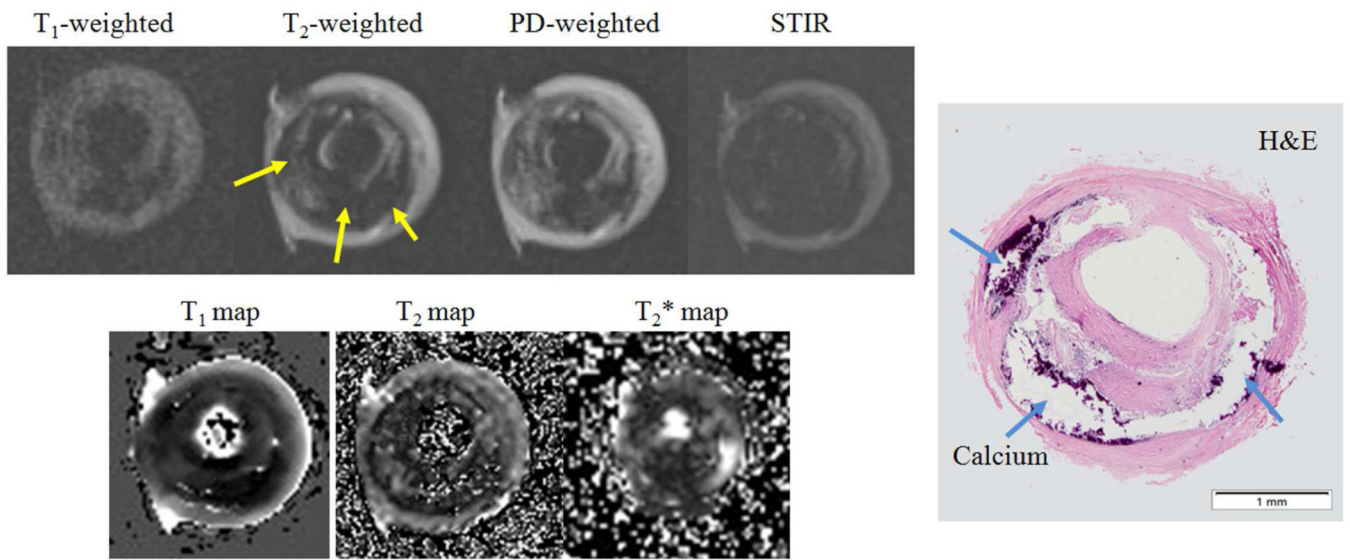
Figure 2.
A heavily calcified middle cerebral artery (MCA) plaque (Type VIII). Arrows show calcification. PD: proton density; STIR: short time inversion recovery. H&E: haematoxylin - eosin.

Table 1

Scanning protocols.

Sequences	T$_1$ Mapping	T$_2$ mapping	T$_2$* mapping	T$_1$-weighted	T$_2$-weighted	PD-weighted	STIR
Type	3D GRE	2D FSE	2D GRE	2D FSE	2D FSE	2D FSE	2D FSE
TR/TE (ms)	15/5.2	2000/18.7–93.5	450/6.4–47.7	581/20	2800/49	2800/20	2000/52
FOV (mm)	50×64	29×45	56×70	39×39	39×39	39×39	39×39
Matrix	250×320	210×320	208×256	384×384	384×384	384×384	384×384
Resolution (mm)	0.2×0.2	0.14×0.14	0.27×0.27	0.1×0.1	0.1×0.1	0.1×0.1	0.1×0.1
Slice thickness (mm)	1	1	1.5	1	1	1	1
Averages	4	4	8	2	3	3	2
Echo train length	1	5	5	4	6	5	6
Number of slices	10 to 48	6 to 36	6 to 24	6 to 48	16 to 48	6 to 48	6 to 30
Scan time	2'40" to 15'0"	17'26" to 34'52"	7'40" to 37'24"	1'51" to 14'48"	8'54" to 26'42"	10'44" to 21'28"	8'28"to 25'24"

TR: time of repetition; TE: echo time; FOV: field of view; GRE: gradient echo; FSE: fast-spin-echo; PD: proton density; STIR: short time inversion recovery.

Table 2

Quantitative mapping results.

	Lipid Core (n=51)	Fibrous Tissue (n=52)	Fibrous Cap (n=48)	Wall (n=22)	Ca (n=22)
T_1 (ms)	519±149	596±146	833±238	632± 123	349±136
T_2 (ms)	69±51	73 ±35	99±76	67± 28	48±28
T_2* (ms)	28±11	30±11	41±15	33± 8	12±5
Proton Density *	1.09±0.35	1.27±0.35	1.37±0.45	1.00±0.24	0.45± 0.21

*
Proton density of the healthy wall was set to 1.00.

Author Manuscript

Author Manuscript

Author Manuscript

Author Manuscript

Table 3

Plaque type classification using MRI compared with histology (Reader 1).

MRI\Histology	Type I,II (13)	Type III (69)	Type IV–V(96)	Type VII (10)	Type VIII (19)
Type I,II (8)	8	0	0	0	0
Type III (62)	5	52	2	0	3
Type IV–V (118)	0	17	91	0	10
Type VII (10)	0	0	0	10	0
Type VIII (9)	0	0	3	0	6

Type I,II: near normal wall thickness; Type III: diffuse intimal thickening or small eccentric plaque with no calcification;
Type IV–V: plaque with a lipid or necrotic core surrounded by fibrous tissue with possible calcification; Type VII: calcified plaque;
Type VIII: fibrotic plaque without lipid core and with possible small calcifications.

Author Manuscript

Author Manuscript

Table 4

Agreement of MRI plaque type classification between readers.

Reader 1 / Reader 2	Type I,II (7)	Type III (74)	Type IV–V (102)	Type VII (10)	Type VIII (14)
Type I,II (8)	7	1	0	0	0
Type III (62)	0	58	1	0	3
Type IV–V (118)	0	15	97	0	6
Type VII (10)	0	0	0	10	0
Type VIII (9)	0	0	4	0	5

Author Manuscript

Author Manuscript